ORIGINAL RESEARCH ARTICLE

Phosphorus Partition Between Liquid Crude Steel and High-Basicity Basic Oxygen Furnace Slags Containing V_2O_5

LUKAS NEUBERT, OLEKSANDR KOVTUN, THILO KRESCHEL, and OLENA VOLKOVA

The influence of V_2O_5 on the phosphorus partition between liquid crude steel and heterogenous basic oxygen furnace (BOF) slag with $CaO/SiO_2 = 4.2$ was investigated at a temperature of 1600 °C in a middle frequency induction furnace. Thereby the phosphorus transfer from "steel to slag" as well as from "slag to steel" was studied over a holding time of 60 minutes. The measured results were shown as phosphorus partition and phosphorus capacity and compared with the experimental values from the literature. It was found that V_2O_5 in highly basic BOF slags decreases phosphorus partition and phosphorus capacity. In addition, the resulting slags were investigated using a scanning electron microscope (SEM).

https://doi.org/10.1007/s11663-023-02778-5

I. INTRODUCTION

VANADIUM is an important alloying element in various steels. As a classic microalloying element, it is used in fine-grained structural steels with contents of < 0.2 mass pct.[1] It has a precipitation-hardening and transformation-retarding effect. However, vanadium has a lower grain refining effect than niobium and titanium. In high-temperature steels and heat-resistant ferritic steels, vanadium is also only used in small quantities < 1 mass pct.[1] It improves mechanical properties such as strength, tempering resistance, wear resistance and hardness. In high-speed steels vanadium is alloyed between 1 and 4 mass pct to increase wear resistance.[1] During the production of vanadium-alloyed steels, the VO_x content in the slag can also increase to up to 5 mass pct.[2] More environmentally friendly iron- and steelmaking, like the direct reduction process with hydrogen, can also increase the VO_x content in the slags. Direct reduced iron (DRI) produced with hydrogen is not comparable to the pig iron currently produced in the blast furnace, due to significantly changed process conditions. The reduction behaviour of the iron ores and the charging materials changes fundamentally, due to a different reducing agent. With hydrogen, a selective reduction process takes place. The iron from the ore is reduced, but most of the components of the gangue are not. Only the pure oxides of molybdenum, nickel and copper can be completely reduced. Especially elements like phosphorus and copper are mostly harmful for the steel and can only be removed with big effort from the melt.[3] Thus, it is possible that oxides like V_2O_5 are retained in increased amounts in direct reduction processes and are later found in the primary metallurgical slag. This is because the reaction between V_2O_5 and H_2 has also a positive change of the standard Gibbs free energy, which is presented in Figure 1. The effect of this modulation regarding the dephosphorisation reaction must be analysed in this context.

Phosphorus is a harmful trace element in steel, which is mainly carried in by the iron ore.[5] It negatively influences the properties of the final steel. For example, high phosphorus concentrations in steel increase the probability of cold fracture, and the weldability, ductility and notched impact strength also decrease. The different steel grades on the market have different requirements for phosphorus content. However, for most steels the phosphorus content is limited to less than 0.045 mass pct.[6,7] The removal of phosphorus from a steel melt can theoretically be described in different ways. On the one hand by an ionic reaction as shown in Eq. [1], on the other hand by a molecular reaction as shown in Eq. [2].[8]

$$[P] + \frac{5}{2}[O] + \frac{3}{2}(O^{2-}) = (PO_4^{3-}) \quad [1]$$

LUKAS NEUBERT, OLEKSANDR KOVTUN, THILO KRESCHEL, and OLENA VOLKOVA are with the Institute of Iron and Steel Technology, TU Bergakademie Freiberg, Leipziger Straße 34, 09599 Freiberg, Germany. Contact e-mail: lukas.neubert@iest.tu-freiberg.de

Manuscript submitted November 30, 2022; accepted March 21, 2023.

Article published online April 19, 2023.

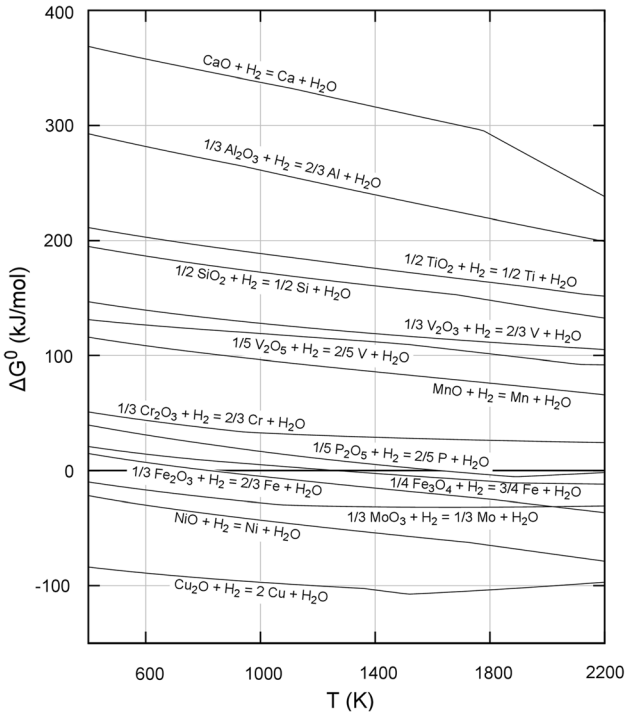

Fig. 1—Change of the standard Gibbs free energy for reactions of hydrogen with different oxides, calculated with FactSage 7.2 (FTOxid, all database).

$$2[\mathrm{P}] + 5[\mathrm{O}] = (\mathrm{P_2O_5}) \quad [2]$$

In the practical steelmaking process, dephosphorisation takes place in the basic oxygen furnace (BOF). The formed P_2O_5 is thermodynamically very unstable and would be reduced again. For this reason, the activity of the P_2O_5 must be reduced for a good dephosphorisation. This is possible by forming compounds with CaO. The real dephosphorisation reaction is shown in Eq. [3]. This also shows that phosphorus does not react with dissolved oxygen, rather with the FeO from the slag.[9]

$$2[\mathrm{P}] + 5(\mathrm{FeO}) + n(\mathrm{CaO}) = (n\mathrm{CaO}\cdot\mathrm{P_2O_5}) + 5[\mathrm{Fe}] \quad [3]$$

A lot of fundamental investigations on the dephosphorization capabilities of liquid primary metallurgical BOF slags or electric arc furnace (EAF) slags were conducted in the past. Thereby the effect of CaO/SiO_2 ratio, FeO_x, MnO, Al_2O_3, MgO, TiO_2 on the phosphorus partition or phosphorus capacity was studied. Several empirical correlations to predict the phosphorus partition or phosphorus capacity as function of temperature, chemical composition of the slags or optical basicity were proposed.[4–8,10–14,16–26] At the same time, unfortunately, very often these correlations work only for slags of the chemical composition for which they were determined.[11] Also, unfortunately, most studies from the past on the removal of phosphorus from crude steel were carried out with liquid slags of low basicity. Real industrial slags used in BOF are most often saturated or oversaturated with CaO, high basic and heterogeneous. Only a few studies have dealt with high basic slags in the past[8,11,21]

The aim of the present work is to investigate the phosphorus partition between the crude steel and high basic BOF slag as a function of V_2O_5 content. Thereby the industrial slag from one European integrated steel plant with the ratio $CaO/SiO_2 = 4.2$ is selected as the initial slag, into which pure V_2O_5 in range up to 15 mass pct is mixed. The samples of slag and steel weighing 25 and 50 g respectively are taken for equilibrium tests. The test time is limited to 60 minutes to assure the minimum infiltration of slag and minimum damage of the MgO crucible. To check the possible achievability of a state close to equilibrium in the present work, equilibrium tests are carried out in both phosphorus transfer directions, ''steel to slag'' and ''slag to steel''.

II. EXPERIMENTAL

A uniform experimental set-up of MFG40 (middle frequency generator) was used for the different test series. It is shown in Figure 2 and is presented in detail in a previous study.[11] Armco iron with 64 ppm of

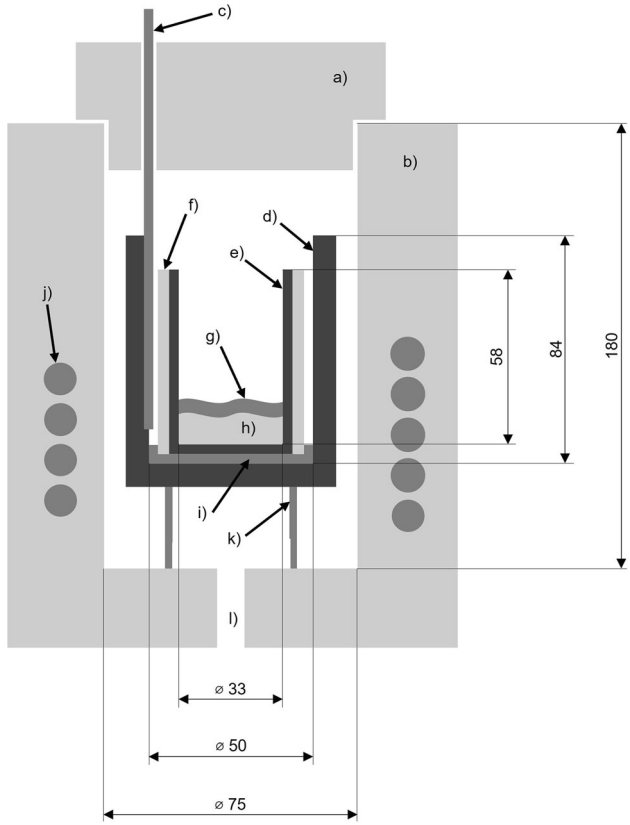

Fig. 2—Experimental set-up of the induction furnace with (*a*) furnace lid, (*b*) furnace chamber, (*c*) thermocouple, (*d*) carbon crucible, (*e*) MgO crucible, (*f*) Al_2O_3 fibre paper, (*g*) slag, (*h*) steel, (*i*) MgO powder, (*j*) inductor, (*k*) ceramic overlay and (*l*) argon flow (measurements in mm).

phosphorus is used for the equilibrium investigations of the phosphorus transfer from slag to steel, the chemical analysis of the Armco iron is shown in Table I. For the equilibrium investigations of the phosphorus transfer from steel to slag the Armco iron is alloyed with FeP25 (17.45 mass pct P, 0.618 mass pct Si, 0.508 mass pct Cr, 0.314 mass pct Al, 0.312 mass pct Ca, 0.055 mass pct Mn, 0.031 mass pct S) up to 790 ppm of phosphorus.

The basis slag comes from one European integrated steel plant. It is ground up to the fraction $< 100\ \mu m$, mixed and pressed into tablets. The chemical analysis of the basis BOF slag is shown in Table II. To study the relationship between phosphorus partition and V_2O_5 content, the experiments are done with 5, 10 and 15 mass pct of V_2O_5 in the slag. Thereby the V_2O_5 with purity of 99.6 pct (Acros Organics) is mixed to the basis slag. Pure, high density 99.8 mass pct MgO, ceramic crucibles (Final Advanced Materials, Bad Bergzabern, Germany) of 60 mm height, and inner and outer diameter of 32 mm and 38 mm, respectively, are used in present work. The MgO crucible is placed in a carbon crucible. For spatial separation between the two crucibles, an Al_2O_3 fibre paper is used on the wall and MgO powder on the bottom. Argon is supplied through a hole in the bottom of the furnace (4 l/min, 99.9990 pct purity) to provide an inert gas atmosphere. The temperature is measured with a type B thermocouple, which is partly located in the carbon crucible. For temperature control, a temperature calibration was periodically done. By measuring the temperature difference between the thermocouple in the carbon crucible and a thermocouple directly in the melt, the right temperature was secured.

The precise compositions of the slags and the phosphorus partition before the experiments are shown in Table III. Certain amounts of V_2O_5, MgO and P_2O_5 are added to a basis slag to create the slags V1–V6. To reduce the wear of the MgO crucibles, the MgO content in all slags was increased up to 10 mass pct. In the first series of experiments, the phosphorus transfer from slag to steel is investigated as a function of different concentrations of V_2O_5. Therefore, the slags V1, V2 and V3 with a high initial phosphorus partition are used. In the second series of experiments, the phosphorus transfer from steel to the slags V4, V5 and V6 with a low initial phosphorus partition is investigated as a function of different concentrations of V_2O_5.

50 g of Armco iron are heated and melted in MFG-40 with a heating rate of 18 K/min. The slag tablet of 25 g is added after a short homogenisation time of about 5 minutes. The melt is hold at 1600 °C for 60 minutes. Cooling takes place in the furnace with about 60 K/min. The entire experimental sequence is shown schematically in Figure 3. Afterwards, the samples of steel and slag are analysed according to their chemical composition. Slag samples are prepared for analysis under the scanning electron microscope (SEM).

III. RESULTS AND DISCUSSION

The chemical composition of the steel and slag after the experiments are shown in Tables IV and V. In addition, Table IV presents the phosphorus partition L_P from the chemical composition after experiments, calculated with Eq. [4], where (P) is the phosphorus content (mass pct) in the heterogeneous slag (respectively the phosphorus content in P_2O_5) and [P] is the phosphorus content (mass pct) in the steel.

$$L_P = \frac{(P)}{[P]} \qquad [4]$$

The results of all the experiments show that the phosphorus partition decreases constantly with increasing content of V_2O_5 in the high basicity slag. This relates to both test series "steel to slag" and "slag to steel". Figure 4 shows this relationship in a diagram. Therefore, it can be assumed that V_2O_5 also reduces the phosphorus capacity of the slag. Figure 5 shows the phosphorus partition additionally as a function of the content of Al_2O_3 and FeO for the same BOF-slag. This research was done also in a previous study.[11] It is shown that under the same process conditions, V_2O_5 behaves in a similarly to Al_2O_3. Both oxides lower the phosphorus partition with increasing concentration. FeO, on the other hand, increases the phosphorus partition if it is present in larger amounts in the slag. However, this effect only occurs at clearly higher concentrations than is the case with V_2O_5 and Al_2O_3.

Pahlevani *et al.* were able to demonstrate a linear relationship between phosphorus content and vanadium content in the pig iron at temperatures and basicities of the slag that differed from those in this study.[27] This dependence also confirms the problematic dephosphorisation in melts with increased vanadium contents. Furthermore, it was confirmed that the activity coefficient of P_2O_5 in the slag is reduced by the addition of V_2O_5. As a result, more phosphorus can be bound in high-temperature phases at increased concentrations of V_2O_5 in the slag.[27]

The phosphorus capacity C_P is defined by the reaction as shown in Eq. [5]. The calculation of the phosphorus capacity is done respectively with Eq. [6] using the mass action law. In general, it is assumed for this calculation that at sufficiently low concentrations, the activity is equal to the concentration or for gases to the partial pressure.

$$\frac{1}{2}\{P_2\} + \frac{5}{4}\{O_2\} + \frac{3}{2}\left(O^{2-}\right) = \left(PO_4^{3-}\right) \qquad [5]$$

$$C_P = \frac{\text{Pct}\, PO_4^{3-}}{p_{P_2}^{\frac{1}{2}} \cdot p_{O_2}^{\frac{5}{4}}} \qquad [6]$$

For comparison, the phosphorus capacity was calculated from an empirical approach (Ap1) according to Eq. [7].[13] This equation also takes into account the content of V_2O_5.

Table I. Chemical Analysis Armco Iron

	C	Si	Mn	P	S	Cr	V
Mass Pct	0.0040	0.0050	0.0202	0.0064	0.0073	0.0030	0.0025

Table II. Chemical Analysis Initial BOF Slag

	CaO	SiO_2	Fe_2O_3	Al_2O_3	MnO	Cr_2O_3	TiO_2	MgO	P_2O_5
Mass Pct	50.73	12.05	26.70	2.04	3.14	0.35	0.81	2.02	2.15

Table III. Chemical Analysis (Mass Pct) and Initial Phosphorus Partition of the Slags Before Experiments

	CaO	SiO_2	Fe_2O_3	MgO	Al_2O_3	MnO	Cr_2O_3	P_2O_5	TiO_2	V_2O_5	L_P
V1	42.34	10.06	22.29	10.00	1.71	2.62	0.30	5.00	0.68	5.00	697.8
V2	39.71	9.43	20.90	10.00	1.60	2.45	0.28	5.00	0.63	10.00	696.9
V3	37.07	8.80	19.50	10.00	1.49	2.29	0.26	5.00	0.59	15.00	695.7
V4	44.01	10.45	23.17	10.00	1.77	2.72	0.31	1.86	0.70	5.00	56.6
V5	41.42	9.84	21.80	10.00	1.67	2.56	0.29	1.75	0.66	10.00	56.5
V6	38.85	9.22	20.44	10.00	1.56	2.40	0.27	1.64	0.62	15.00	56.4

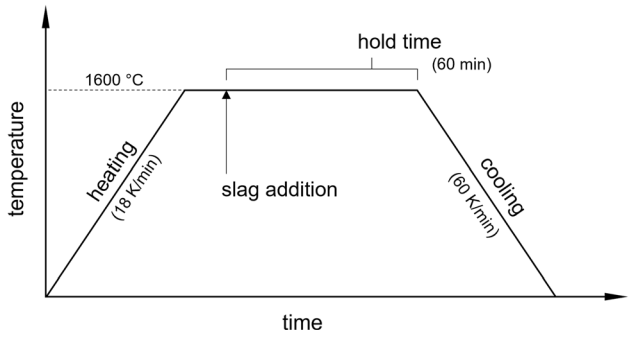

Fig. 3—Schematic experimental sequence.

$$\log(C_P) = \frac{46141}{T} + 0.020(\text{CaO}) - 0.010(\text{MgO}) - 0.077(\text{P}_2\text{O}_5) - 0.102(\text{SiO}_2) - 0.059(\text{Fe}_t\text{O}) - 0.040(\text{MnO}) - 0.084(\text{Al}_2\text{O}_3) - 0.079(\text{TiO}_2) - 0.080(\text{V}_2\text{O}_5) - 3.475 \quad [7]$$

The partial pressures of phosphorus and oxygen are defined by Eqs. [8] and [10]. The calculation is done with the equilibrium constants of the respective reactions, as shown in Eqs. [9] and [11].

$$\frac{1}{2}\{\text{P}_2\} = [\text{P}] \quad [8]$$

$$K_P = \frac{\text{Pct P}}{p_{\text{P}_2}^{\frac{1}{2}}} \quad [9]$$

$$\frac{1}{2}\{\text{O}_2\} = [\text{O}] \quad [10]$$

$$K_O = \frac{\text{Pct O}}{p_{\text{O}_2}^{\frac{1}{2}}} \quad [11]$$

Different approaches can be used to determine the equilibrium constants K_P and K_O. Equations [12] and [13] were used for the first calculation of the phosphorus capacity (Ap2).[13] Equations [14] and [15] were used for another calculation approach (Ap3).[14,15]

Table IV. Chemical Analysis (Mass Pct) and Phosphorus Partition of the Steels After Experiments

	C	Si	Mn	P	S	Cr	V	L_P
V1a	0.0057	0.0050	0.0310	0.0048	0.0129	0.0030	0.0020	455.13
V1b	0.0059	0.0050	0.0277	0.0046	0.0121	0.0030	0.0020	494.09
V2a	0.0067	0.0050	0.0270	0.0077	0.0148	0.0030	0.0035	261.43
V2b	0.0074	0.0050	0.0290	0.0066	0.0151	0.0030	0.0033	311.62
V3a	0.0066	0.0050	0.0226	0.0124	0.0166	0.0030	0.0059	161.18
V3b	0.0096	0.0050	0.0218	0.0119	0.0168	0.0030	0.0042	161.14
V4a	0.0056	0.0050	0.0366	0.0024	0.0099	0.0030	0.0022	414.23
V4b	0.0064	0.0050	0.0396	0.0027	0.0109	0.0038	0.0020	368.44
V5a	0.0060	0.0050	0.0312	0.0025	0.0117	0.0041	0.0023	356.03
V5b	0.0078	0.0050	0.0313	0.0025	0.0118	0.0041	0.0025	347.42
V6a	0.0052	0.0050	0.0299	0.0041	0.0137	0.0056	0.0059	192.85
V6b	0.0055	0.0050	0.0280	0.0052	0.0140	0.0030	0.0058	147.21

Table V. Chemical Analysis (Mass Pct) and Basicity of the Slags After Experiments

	CaO	SiO_2	Fe_2O_3	MgO	Al_2O_3	MnO	Cr_2O_3	P_2O_5	TiO_2	V_2O_5	CaO/SiO_2
V1a	38.18	9.20	27.40	9.74	2.35	2.18	0.43	4.86	0.62	5.04	4.15
V1b	38.68	9.41	26.52	9.74	2.22	2.18	0.44	5.06	0.62	5.13	4.11
V2a	35.45	8.28	28.39	9.65	1.85	1.94	0.57	4.47	0.54	8.86	4.28
V2b	37.12	8.62	26.25	9.49	1.90	1.99	0.58	4.58	0.56	8.91	4.30
V3a	32.42	7.35	29.12	9.82	1.49	1.75	0.69	4.44	0.49	12.43	4.41
V3b	32.88	7.50	27.45	10.30	1.74	1.84	0.71	4.27	0.50	12.81	4.38
V4a	40.63	10.06	26.84	9.32	2.42	2.26	0.44	2.21	0.64	5.18	4.04
V4b	40.86	10.17	26.72	9.25	2.28	2.26	0.44	2.22	0.65	5.15	4.02
V5a	37.32	9.23	26.33	10.77	1.82	2.12	0.60	1.99	0.57	9.25	4.05
V5b	37.78	9.19	26.77	9.72	2.22	2.10	0.58	1.94	0.59	9.11	4.11
V6a	33.92	7.71	28.14	10.33	2.03	1.81	0.71	1.76	0.53	13.06	4.40
V6b	33.84	7.67	28.28	10.34	2.31	1.80	0.70	1.70	0.52	12.84	4.41

$$K_P^{\text{Drain (Ref 13)}} = e^{\frac{\Delta G_P^0}{-RT}} = e^{\frac{-122{,}173+19.25T}{-RT}} \quad [12]$$

$$K_O^{\text{Drain (Ref 13)}} = e^{\frac{\Delta G_O^0}{-RT}} = e^{\frac{-115{,}750+4.63T}{-RT}} \quad [13]$$

$$K_P^{\text{Maruoka (Ref 14)}} = e^{\frac{\Delta G_P^0}{-RT}} = e^{\frac{-155{,}700+5.4T}{-RT}} \quad [14]$$

$$K_O^{\text{Oeters(Ref 15)}} = 10^{\frac{5832}{T}+0.356} \quad [15]$$

The phosphorus capacities decrease with increasing V_2O_5 content in both test series, as it is shown in Figure 6. This also confirms the relationship between phosphorus partition and V_2O_5 content. The experiments on phosphorus transfer from slag to steel show lower phosphorus capacities overall than in the experiments on phosphorus transfer from steel to slag. As a result, less phosphorus can be removed from the melt during steel production with increased vanadium contents in the slag. This requires special attention in order not to reduce the quality of the finished product and still set the desired phosphorus contents. The higher phosphorus capacities achieved in the phosphorus transfer from steel to slag are useful, as only this transport direction is crucial for dephosphorisation.

Afterwards, the slags are analysed using SEM (AsB detector). Figures 7 and 8 show different SEM images of the slags produced with varying V_2O_5 content from the test series ''slag to steel''. Different phases, which differ in their brightness, can be observed in the solid slag (B1, B2 and B3). The simulation with FactSage 7.2 (FTOxid, all database) at experimental temperature and standard pressure shows, in accordance with the EDX analysis, one solid phase and two liquid phases in the slags. The solid phase is of the type $3CaO{\cdot}V_2O_5$ and can be assigned to phase B2. The other calculated liquid phases in the slags could be B1 and B3. The calculated liquid slag phases differ in their chemical composition. The first calculated liquid phase is rich in CaO, SiO_2, P_2O_5 and V_2O_5 and thus, similar to B3. The second calculated liquid phase should be the residual liquid slag, without P_2O_5 and V_2O_5 and is similar to B1. The proportion of phases in the microstructure was determined graphically with a software (OLYMPUS Stream Motion).

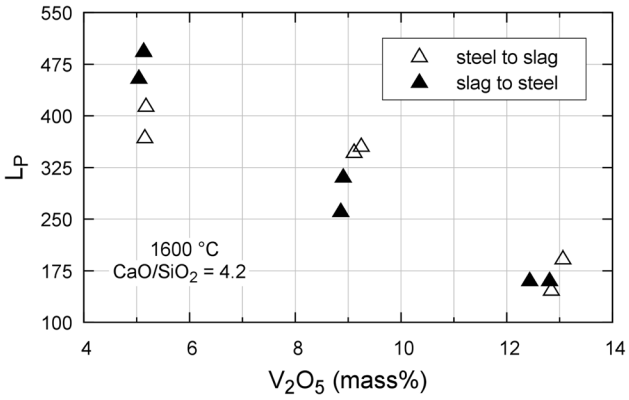

Fig. 4—Phosphorus partition as a function of the content of V_2O_5 at 1600 °C.

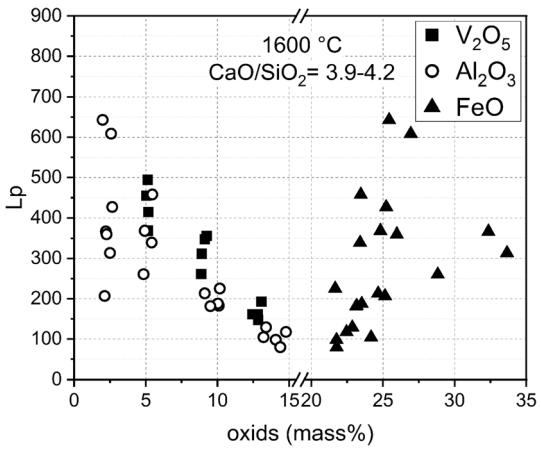

Fig. 5—Phosphorus partition as a function of the content of Al_2O_3,[11] FeO[11] and V_2O_5 at 1600 °C.

According to EDX analysis, B1 consists mainly of iron, oxygen, magnesium, manganese and calcium and is present in almost equal proportions in the microstructure, irrespective of the V_2O_5 content. The chemical composition of B2 is dominated by calcium, vanadium and oxygen, which form calcium vanadates. Iron and aluminium also occur in B2. The proportion of B2 increases strongly with increasing V_2O_5 contents in the slag. In B3, phosphorous is mainly bound in the form of calcium phosphates. EDX analysis confirms that this phase consists mostly of calcium, silicon, phosphorus and oxygen. In addition, vanadium also enriches in B3. Phosphorus and vanadium can be bound both in the phase B3. Due to increasing contents of V_2O_5 in the slag, the phosphorus partition decreases, as vanadium displaces the element phosphorus from B3 phase. Simultaneously, the phosphorus capacity of the slag decreases. With increasing contents of V_2O_5, the amount of phase B3 in the microstructure decreases, respectively.

All experiments were simulated with FactSage 7.2 (FTOxid, all database). The results of the simulation show the fractions of B1, B2 and B3 in the slag that can be observed in the SEM. The concrete results are shown in Table VI. According to this, the proportion of B1 and B2 increases with increasing V_2O_5 content and B3 decreases with increasing V_2O_5 content. This trend could be confirmed through the experiments.

The simulation of the different vanadium-containing slags at experimental conditions shows that solid calcium vanadates of the type $3CaO{\cdot}V_2O_5$ exist in the liquid slags, which represent the observed phase B2. There is no $3CaO{\cdot}V_2O_5$ phase in the initial basic BOF slag. The $3CaO{\cdot}V_2O_5$ phase will bind CaO from the slag. According to Eq. [3], less phosphorus can be removed from the melt and the phosphorus partition decreases.

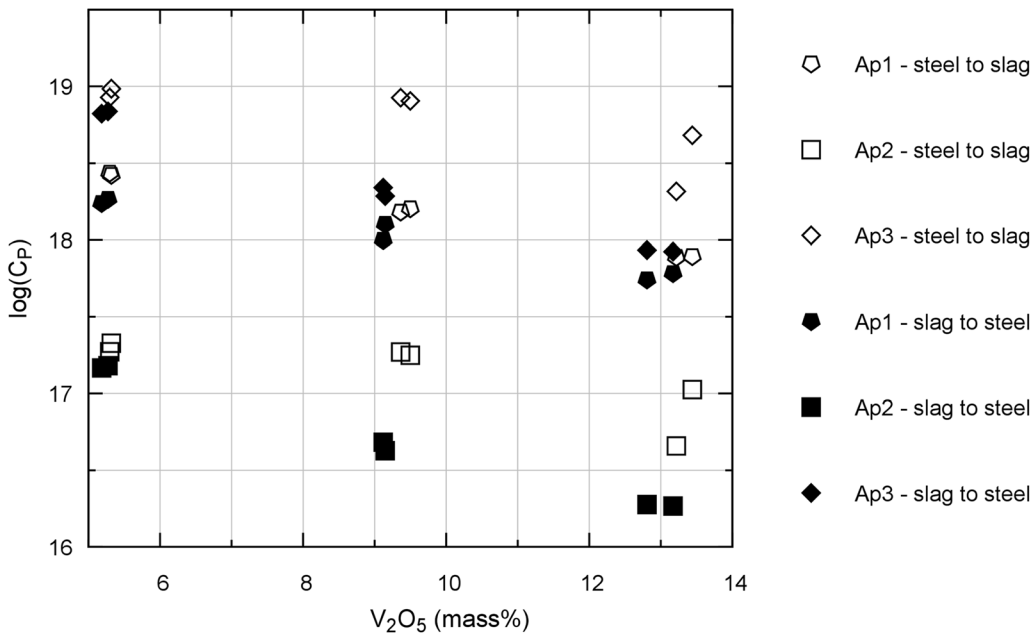

Fig. 6—Phosphorus capacity (logarithmic) as a function of the content of V_2O_5 at 1600 °C.

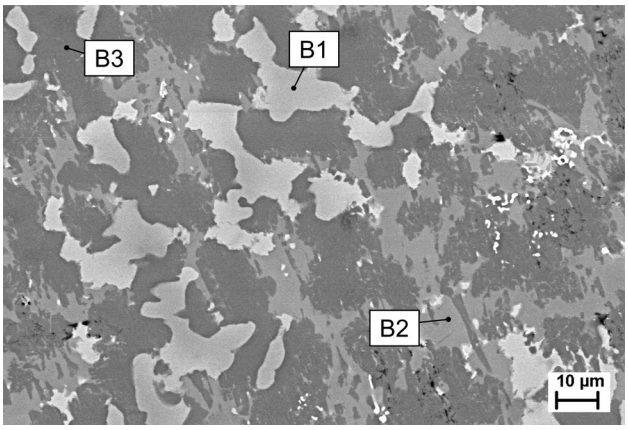

Fig. 7—SEM image of the slag from V1b where $V_2O_{5,initial}$ = 5mass pct (Phase proportion of B1 = 23.31 pct, B2 = 19.7 pct, B3 = 56.59 pct).

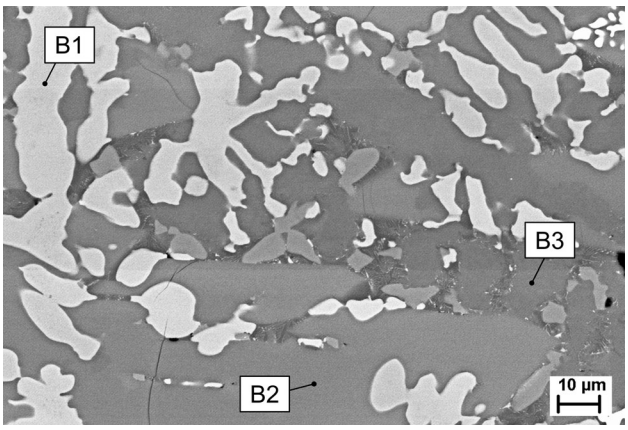

Fig. 8—SEM image of the slag from V3b where $V_2O_{5,initial}$ = 15mass pct (Phase proportion of B1 = 25.22 pct, B2 = 68.6 pct, B3 = 5.86 pct).

Phosphorus gathers at 1600 °C preferentially in the liquid phase B3, which is also rich in CaO and SiO_2. With increasing contents of V_2O_5 in the slag, vanadium displaces the phosphorus in B3. This mechanism could also reduce the phosphorus partition.

IV. CONCLUSION

The influence of V_2O_5 on the phosphorus partition between a highly basic BOF slag and a steel melt was confirmed. It is shown that the phosphorus partition decreases with increasing contents of V_2O_5 in the slag. This seems to be almost independent of whether the phosphorus transfer from slag to steel or the phosphorus transfer from steel to slag was investigated. In both cases, phosphorus partitions between 150 and 160 could be achieved at a temperature of 1600 °C with an addition of 15 mass pct V_2O_5 and 1 hour holding time. The initial phosphorus partition was just under 700 in the ''slag to steel'' experiments and around 56 in the ''steel to slag'' experiments. Also, the phosphorus capacity of the slag decreases with increasing contents of V_2O_5. The evaluation of the slags obtained in the SEM shows in which phases phosphorus is bound in the slag. Vanadium displaces phosphorus from a liquid slag phase, which is also rich in CaO and SiO_2. In addition, the solid phase of the type $3CaO{\cdot}V_2O_5$ exists with increasing contents of V_2O_5 more frequent at experimental conditions. In this case, more CaO, which is necessary for dephosphorisation, is bound. These facts confirm the decreasing effect of V_2O_5 in the slag on the phosphorus partition.

Table VI. Calculated Fractions (Mass Pct) of B1, B2 and B3 in the Slag

	B1	B2	B3
V1	9.36	9.55	78.32
V2	9.51	15.35	71.35
V3	11.08	16.71	69.81
V4	9.10	12.37	74.28
V5	10.28	20.31	63.05
V6	11.50	22.50	60.49

ACKNOWLEDGEMENTS

The investigation was supported by the German Research Foundation (DFG). The authors are grateful for the financial support and helpful discussion within the framework of the GRK 2802 (P4). Thanks are also due to the technical staff of the Institute of Iron and Steel Technology of the TU Bergakademie Freiberg.

CONFLICT OF INTEREST

The authors declare that they have no conflict of interest.

FUNDING

Open Access funding enabled and organized by Projekt DEAL.

REFERENCES

1. W. Bleck and E. Moeller: *Handbuch Stahl*, Hanser, München, 2018.
2. S. Seetharaman, T. Shyrokykh, C. Schröder, and P.R. Scheller: *Metall. Mater. Trans. B*, 2013, vol. 44B, pp. 783–88.
3. B. Li, G. Sun, S. Li, H. Guo, and J. Guo: *Materials*, 2020, vol. 13, p. 842.
4. A.N. Assis, M.A. Tayeb, S. Sridhar, and R.J. Fruehan: *Metall. Mater. Trans. B*, 2015, vol. 46B, pp. 2255–63.
5. J. Huss, M. Berg, and N. Kojola: *Metall. Mater. Trans. B*, 2020, vol. 51B, pp. 786–94.
6. H. Xue, J. Li, Y. Xia, Y. Wan, L. Chen, and C. Lv: *Metals*, 2021, vol. 11, p. 216.
7. J. Li, S.-J. Wang, Y.-J. Xia, and H. Kong: *Ironmak. Steelmak.*, 2015, vol. 42, pp. 70–73.
8. P.B. Drain, B.J. Monaghan, R.J. Longbottom, M.W. Chapman, G. Zhang, and S.J. Chew: *ISIJ Int.*, 2018, vol. 58, pp. 1965–71.
9. H. W. Gudenau: *Metallurgie – Materialsammlung zum Praktikum Metallurgie*, RWTH Aachen, 2002.
10. M. Lv, R. Zhu, and L. Yang: *Steel Res. Int.*, 2019, vol. 90, p. 1800454.
11. O. Kovtun, M. Karbayev, I. Korobeinikov, C. Srishilan, A.K. Shukla, and O. Volkova: *Steel Res. Int.*, 2021, vol. 92, p. 2000607.
12. B. Deo, J. Halder, B. Snoeijer, A. Overbosch, and R. Boom: *Ironmak. Steelmak.*, 2005, vol. 32, pp. 54–60.
13. P.B. Drain, B.J. Monaghan, R.J. Longbottom, M.W. Chapman, G. Zhang, and S.J. Chew: *ISIJ Int.*, 2019, vol. 59, pp. 839–47.
14. N. Maruoka, S. Ono, H. Shibata, and S. Kitamura: *ISIJ Int.*, 2013, vol. 53, pp. 1709–14.
15. F. Oeters: *Metallurgie der Stahlherstellung*, Springer, Berlin, 1989, p. 18.
16. A. Basu, A.K. Lahiri, and S. Seetharaman: *Metall. Mater. Trans. B*, 2007, vol. 38B, pp. 357–66.
17. A. Basu, A.K. Lahiri, and S. Seetharaman: *Metall. Mater. Trans. B*, 2007, vol. 38B, pp. 623–30.
18. A. Basu, S. Seetharaman, and A.K. Lahiri: *Steel Res. Int.*, 2010, vol. 81, pp. 932–39.
19. J.D. Zhou, X.G. Bi, and F. Yang: *Ironmak. Steelmak.*, 2014, vol. 41, pp. 298–303.
20. H. Suito and R. Inoue: *ISIJ Int.*, 1995, vol. 35, pp. 266–71.
21. E. Schuermann and H. Fischer: *Steel Res.*, 1991, vol. 62, pp. 303–13.
22. A.N. Assis, M. Tayeb, S. Sridhar, and R.J. Fruehan: *MDPI Met.*, 2019, vol. 9, p. 116.
23. H. Suito and R. Inoue: *Trans. ISIJ*, 1984, vol. 24, pp. 40–46.
24. H. Suito and R. Inoue: *ISIJ Int.*, 1995, vol. 35, pp. 258–65.
25. A. N. Assis, R. J. Fruehan, S. Sridhar: in *AISTech, Iron and Steel Technology Conference and Exposition*, Atlanta, GA, 2012, pp. 861–70.
26. K. Ide and R.J. Fruehan: *Iron Steelmaker*, 2000, vol. 27(12), pp. 65–70.
27. F. Pahlevani, H. Shibata, N. Maruoka, S. Kitamura, and R. Inoue: *ISIJ Int.*, 2011, vol. 51, pp. 1624–30.